El-Asmy *et al. Chemistry Central Journal (2015) 9:69*
DOI 10.1186/s13065-015-0135-y

Chemistry Central Journal

RESEARCH ARTICLE Open Access

Spectral, thermal, molecular modeling and biological studies on mono- and binuclear complexes derived from oxalo bis(2,3-butanedionehydrazone)

Ahmed El-Asmy*, Bakir Jeragh and Mayada Ali

Abstract

Background: Hydrazones and their metal complexes were heavily studied due to their pharmacological applications such as antimicrobial, anticonvulsant analgesic, anti-inflammatory and anti-cancer agents. This work aims to synthesize and characterize novel complexes of VO^{2+}, Co^{2+}, Ni^{2+}, Cu^{2+}, Zn^{2+}, $Zr^{4+}$and Pd^{2+} ions with oxalo bis(2,3-butanedione-hydrazone). Single crystals of the ligand have been grown and analyzed.

Results: Oxalo bis(2,3-butanedionehydrazone) [OBH] has a monoclinic crystal with P 1 21/n 1 space group. The VO^{2+}, Co^{2+}, Ni^{2+}, Cu^{2+}, Zn^{2+}, Zr^{4+} and Pd^{2+} complexes have the formulas: $[VO(OBH–H)_2]\cdot H_2O$, $[Co(OBH)_2Cl]Cl\cdot ½EtOH$, $[Ni_2(OBH)Cl_4]\cdot H_2O\cdot EtOH$, $[Cu(OBH)_2Cl_2]\cdot 2H_2O$, $[Zn(OBH–H)_2]$, $[Zr(OBH)Cl_4]\cdot 2H_2O$, and $[Pd_2(OBH)(H_2O)_2Cl_4]\cdot 2H_2O$. All complexes are nonelectrolytes except $[Co(OBH)_2Cl]Cl\cdot ½EtOH$. OBH ligates as: neutral tetradentate (NNOO) in the Ni^{2+} and Pd^{2+} complexes; neutral bidentate (OO) in $[Co(OBH)_2Cl]Cl\cdot ½EtOH$, $[Zr(OBH)Cl_4]\cdot 2H_2O$ and $[Cu(OBH)_2Cl_2]\cdot 2H_2O$ and monobasic bidentate (OO) in the Zn^{2+} and VO^{2+} complexes. The NMR (^1H and ^{13}C) spectra support these data. The results proved a tetrahedral for the Zn^{2+} complex; square-planar for Pd^{2+}; mixed stereochemistry for Ni^{2+}; square-pyramid for Co^{2+} and VO^{2+} and octahedral for Cu^{2+} and Zr^{4+} complexes. The TGA revealed the outer and inner solvents as well as the residual part. The molecular modeling of $[Ni_2(OBH)Cl_4]\cdot H_2O\cdot EtOH$ and $[Co(OBH)_2Cl]Cl\cdot ½EtOH$ are drawn and their molecular parameters proved that the presence of two metals stabilized the complex more than the mono metal. The complexes have variable activities against some bacteria and fungi. $[Zr(OBH)Cl_4]\cdot 2H_2O$ has the highest activity. $[Co(OBH)_2Cl]Cl\cdot ½EtOH$ has more activity against *Fusarium*.

Conclusion: Oxalo bis(2,3-butanedionehydrazone) structure was proved by X-ray crystallography. It coordinates with some transition metal ions as neutral bidentate; mononegative bidentate and neutral tetradentate. The complexes have tetrahedral, square-planar and/or octahedral structures. The VO^{2+} and Co^{2+} complexes have square-pyramid structure. $[Cu(OBH)_2Cl_2]\cdot 2H_2O$ and $[Ni_2(OBH)Cl_4]\cdot H_2O\cdot EtOH$ decomposed to their oxides while $[VO(OBH–H)_2]\cdot H_2O$ to vanadium. The energies obtained from molecular modeling calculation for $[Ni_2(OBH)Cl_4]\cdot H_2O\cdot EtOH$ are less than those for $[Co(OBH)_2Cl]Cl\cdot ½EtOH$ indicating the two metals stabilized the complex more than mono metal. The Co(II) complex is polar molecule while the Ni(II) is non-polar.

*Correspondence: aelasmy@yahoo.com
Chemistry Department, Faculty of Science, Kuwait University, 5969, Kuwait city, Safat 1360, Kuwait

Graphical abstract:

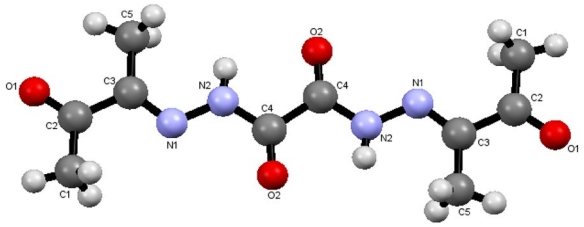

Crystal structure of oxalo bis(2,3-butanedionehydrazone)

Keywords: Hydrazones, Spectra, TGA, Biological activity, X-ray crystallography

Background

Hydrazones and their metal complexes are heavily studied compounds which have many pharmacological applications such as antimicrobial, anticonvulsant analgesic, anti-inflammatory and anti-cancer agents. Acetylpyridine and benzoylpyridine hydrazones were used as reagents against brain tumor and are highly cytotoxic to glioma cells [1]. Interest has been focused on hydrazone complexes to study their anti-parasitic, fungicidal and bactericidal properties [2, 3]. 2,3-Butanedione monoxime possessed cardio protective properties related to the inhibition of cross-bridge force development [4]. Heterocyclic compounds containing nitrogen have much attention due to their activity as antitumor, anti-inflammation, anti-pyretic, antiviral, anti-microbial, insecticides and fungicides [5–7]. Isonicotinyl hydrazone complexes of 2-acetylpyridine, pyrrolyl-2-carboxaldehyde, 2,5-dihydroxy-acetophenone, N-isonicotinamido-furfuraldimine, 2-thiophenecarbonyl and 3-(N-methyl)-isatin were reported [8–12]. The Ni(II) and Cu(II) complexes of 2,3-butanedione bis(N(3)substituted-thiosemicarbazones) were studied and some of these compounds were solved by x-ray crystallography [13]. The crystal structures of [Cu(HxPip-2H)] (HxPip = 3,4-hexanedione bis(3-piperidylthiosemicarbazone) and [Cu(HxHexim-2H)] (HxHexim = 3,4-hexanedione bis(3-hexa-methyleneiminylthiosemicarbazone) were solved having a square-planar geometry [14]. Binuclear complexes of VO^{2+}, Co^{2+}, Ni^{2+}, Cu^{2+} and Zn^{2+} with oxalyl bis(diacetylmonoximehydrazone) were characterized as 2:2 (M:L) and an octahedral geometry for VO^{2+}, tetrahedral for Zn^{2+} and square-planar for the rest complexes were proposed [15]. On continuation to our work on bis(hydrazones) and their complexes [16, 17], this work aims to synthesize and characterize novel complexes of VO^{2+}, Co^{2+}, Ni^{2+}, Cu^{2+}, Zn^{2+}, $Zr^{4+}$and Pd^{2+} ions with oxalo bis(2,3-butanedione-hydrazone). Single crystals for the ligand have been grown and analyzed. Trials to grow crystals for the complexes were failed, so molecular modeling for the Co(II) and Ni(II) complexes were done.

Experimental

$VOSO_4{\cdot}2H_2O$, $CoCl_2{\cdot}6H_2O$, $NiCl_2{\cdot}6H_2O$, $CuCl_2{\cdot}2H_2O$, $ZnCl_2{\cdot}2H_2O$, K_2PdCl_4 and $ZrCl_4$, diethyl oxalate, hydrazine hydrate, 2,3-butanedione, ethanol, diethyl ether, DMF and DMSO were obtained from the BDH chemicals.

Synthesis of oxalo bis(2,3-butanedionehydrazone) [OBH]

OBH was prepared by heating under reflux a suspension (6 g, 0.05 mol) of oxalic acid dihydrazide in 50 mL EtOH and 8.6 ml (0.1 mol) of 2,3-butanedione on a heating mantle for 10 h. The precipitate thus formed was filtered off, recrystallized from ethanol and finally dried. It was characterized by elemental analysis and spectral studies. The ^{1}H NMR spectrum of the ligand showed signals at $\delta = 11.924$ (s, 2H) and 2.129 (s, 6H) ppm for the NH and CH_3 protons. Its ^{13}C NMR showed peaks at 196.65, 167.58, 148.81 and 23.90 ppm for $(C{=}O)_{ketonic}$ $(C{=}O)_{amidic}$, C=N and CH_3, respectively.

Preparation of the metal complexes

The metal complexes were prepared by reacting calculated amounts corresponding to 2:1 ratio [M:L] in 50 mL EtOH and the mixture was heated under reflux for 6–8 h. In the preparation of VO^{2+} complex, 0.1 g of sodium acetate was added to raise the pH (~8) and precipitating the complex. The formed precipitates were filtered off, washed with hot water, hot ethanol and diethyl ether and finally dried in a vacuum desiccator over anhydrous silica gel. Attempts to grow single crystals for the complexes were done but unsuccessful.

Analysis and equipment

Carbon, hydrogen and nitrogen content of the compounds were determined at the Microanalytical Unit (Varian Micro V1.5.8, CHNS Mode, 15073036) of Kuwait University. The metal content was determined using ICP-OES GBC Quantium Sequential at Kuwait University. The mass spectra were recorded on a GC–MS Thermo-DFS (BG_FAB) mass spectrometer. The

melting points were measured on a Griffin melting point apparatus. The conductance for 10^{-3} mol L^{-1} DMSO solution of the compounds was measured on Orion 3 STAB Conductivity Bridge. The IR spectra were recorded as KBr discs on a FT/IR-6300 type A (400–4000 cm^{-1}). The electronic spectra of the complexes were recorded on a Cary 5 UV–vis spectrophotometer, varian (200–900 nm). The ^1H NMR spectra of the ligand and the diamagnetic complexes were recorded in DMSO-d6, on a Bruker WP 200 SY Spectrometer (400 MHz) at room temperature using tetramethylsilane (TMS) as an external standard. The magnetic measurements were carried out on a Johnson-Matthey magnetic balance, UK. The TGA thermograms were recorded (25–800 °C) on a Shimadzu TGA-60; the nitrogen flow and heating rate were 50 ml/min and 10 °C min^{-1}, respectively. The X-ray single crystal diffraction data were collected on a Rigaku R-Axis Rapid diffractometer using filtered Mo-K α-radiation. The structure was solved by the direct methods and expanded using Fourier techniques at Kuwait University. The ligand and its complexes were investigated for antimicrobial activity against *Bacillus, Aspergillus, Escherichia coli, Penicillium* and *Fusarium* as reported earlier [15]. All molecular calculations were carried out by HyperChem 7.51 software package. The molecular geometry of the Co^{2+} and Ni^{2+} complexes are first optimized at molecular mechanics (MM+) level. Semi empirical method PM3 is then used for optimizing the full geometry of the system using Polak–Ribiere (conjugate gradient) algorithm and Unrestricted Hartee-Fock (UHF) is employed keeping RMS gradient of 0.01 kcal/Å mol.

Results and discussion

Crystal analysis of OBH

The crystal structure of OBH is shown in Structure 1. Its refinement data are summarized in Table 1 while the bond lengths and bond angles are presented in Table 2. OBH was crystalized as monoclinic system and P 121/n1 space group with molecular weight of 254.25. The N_1–C_3, O_1–C_2 and O_2–C_4 distances are 1.283(3), 1.210(3) and 1.206 Å, respectively, indicating true double bond; the amidic carbonyl has value slightly higher than the ketonic carbonyl. The N_2–C_4 and N_1–N_2 are 1.351(4) and 1.381 Å indicating single bonds. All bond angles are between 115 and 127 and 109.5° meaning the trigonal and tetrahedral geometries with sp^2 and sp^3 hybridization. The presence of lone pair of electrons on N_1 in $C_3N_1N_2$ reduces the angle from 120° to 115.7°. The bond angle of N_2–C_4–C_4 reduces to 110.6°, in consistent with some distortion, while that of O_2–C_4–N_2 increases to 126.9° due to the existence of two more electronegative atoms (O atoms).

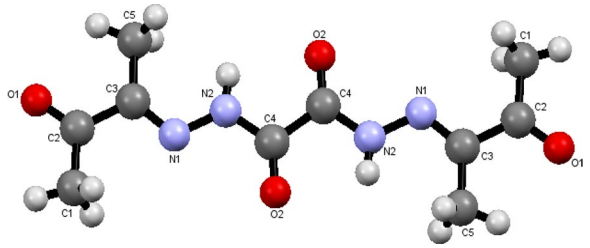

Structure 1 Crystal structure of oxalo bis(2,3-butanedionehydrazone)

Table 1 Crystallographic data for OBH crystal

Identification code	OBH
Chemical formula	$C_{10}H_{14}N_4O_4$
Formula weight	254.25
Temperature	296 (2) K
Wavelength	1.54178 Å
Crystal size	0.020 × 0.120 × 0.230 mm
Crystal habit	Clear light colorless flakes
Crystal system	Monoclinic
Space group	P 1 21/n 1
Unit cell dimensions	a = 6.3630 (5) Å, α = 90° b = 4.6609 (4) Å, β = 91.37° c = 20.7562 (19) Å, γ = 90°
Volume	615.40 (9) $Å^3$
Z	2
Density (calculated)	1.372 g/cm^3
Absorption coefficient	0.915 mm^{-1}
F (000)	268

Analytical data

The data of CHN and metal contents of the complexes are presented in Table 3. The values confirm mononuclear complexes: $[VO(OBH–H)_2]\cdot H_2O$, $[Co(OBH)_2Cl]Cl\cdot ½EtOH$, $[Cu(OBH)_2Cl_2]\cdot 2H_2O$, $[Zn(OBH–H)_2]$, $[Zr(OBH)Cl_4]\cdot 2H_2O$ and binuclear complexes: $[Ni_2(OBH)Cl_4]\cdot H_2O\cdot EtOH$ and $[Pd_2(OBH)(H_2O)_2Cl_4]\cdot 2H_2O$. All complexes are colored, solid and stable towards air and moisture at room temperature. They have high melting points and are insoluble in most common organic solvents and completely soluble in DMSO. The molar conductance values (Table 3) of 10^{-3} mol L^{-1} DMSO solution proved the non-electrolytic nature. The measured value for the Co(II) complex supports the formation of $[Co(OBH)_2Cl]^+Cl^-\cdot ½EtOH$ [18].

IR and NMR (^1H and ^{13}C) spectra

OBH showed the characteristic bands for ν(NH), ν(C=O) [ketonic and amidic] and ν(C=N) vibrations at 3325, 1701 and 1605, respectively in its IR spectrum (Fig. 1a).

Table 2 Bond lengths and bond angles of OBH

Bond	Length	Bond	Length
O1–C2l	1.210 (3)	O2–C4	1.206 (3)
N1–C3	1.283 (3)	N1–N2	1.381 (3)
N2–C4	1.351 (4)	N2–H7	0.86
C1–C2	1.479 (4)	C1–H1	0.96
C1–H2	0.96	C1–H3	0.96
C2–C3	1.506 (4)	C3–C5	1.486 (4)
C4–C4#1	1.529 (6)	C5–H5	0.96
C5–H4	0.96	C5–H6	0.96
Bond	**Angle (°)**	**Bond**	**Angle (°)**
C3–N1–N2	115.7 (2)	C4–N2–N1	120.6 (2)
C4–N2–H7	119.7	N1–N2–H7	119.7
C2–C1–H1	109.5	C2–C1–H2	109.5
H1–C1–H2	109.5	C2–C1–H3	109.5
H1–C1–H3	109.5	H2–C1–H3	109.5
O1–C2–C1	122.0 (3)	O1–C2–C3	117.9 (3)
C1–C2–C3	120.1 (3)	N1–C3–C5	126.6 (3)
N1–C3–C2	115.0 (3)	C5–C3–C2	118.4 (3)
O2–C4–N2	126.9 (3)	O2–C4–C4#1	122.4 (3)
N2–C4–C4#1	110.6 (3)	C3–C5–H5	109.5
C3–C5–H4	109.5	H5–C5–H4	109.5
C3–C5–H6	109.5	H5–C5–H6	109.5
H4–C5–H6	109.5		

Inspections of the IR spectral data of the complexes, Table 4, three modes are suggested. The ^{1}H NMR spectrum showed the NH and CH_3 protons at 11.924 (s, 2H) and 2.129 (s, 6H) ppm, respectively. On the other hand, the ^{13}C NMR spectrum have multiple peaks corresponding to $(C{=}O)_{ketoni}$, $(C{=}O)_{amidic}$, C=N and CH3 groups at 196.65, 167.58, 148.81 and 23.90 ppm.

In the first mode, OBH acts as a neutral bidentate ligand in $[Co(OBH)_2Cl]Cl{\cdot}½EtOH$ (Structure 2), $[Cu(OBH)_2Cl_2]{\cdot}2H_2O$ and $[Zr(OBH)Cl_4]{\cdot}2H_2O$ coordinating through the two amidic carbonyl groups based on the following observations: the υ(C=O) band observed at 1701 cm^{-1} in ligand spectrum was shifted to 1686–1699 cm^{-1} in complexes having little intensity indicating that the two amidic carbonyl groups ($C{=}O_{amidic}$) participated in bonding while the other two carbonyl ($C{=}O_{ketonic}$) still at the same position. The new band at 464–495 cm^{-1} is due to υ(M–O) vibration [19]. The υ(C=N) at 1605 cm^{-1} appeared very weak, less intensity with little shift to higher wavenumber in the Co(II) and Cu(II) complexes and to lower wavenumber in the Zr(IV) complex (1585 cm^{-1}).

In the second mode, OBH acts as a mononegative bidentate in Zn^{2+} and VO^{2+} complexes coordinating through the two amidic carbonyl (enolic form), from each ligand molecule. The shift of υ(C=O) to lower or higher wavenumbers with appearance of υ(C=N)*, υ(C–O) (due to enolization of one amidic group) [20] and υ(M–O) at 1550, 1140 and 463 cm^{-1} indicates the participation of carbonyl group in bonding. In the VO^{2+} complex, the band observed at 3412 cm^{-1} is attributed to hydrated water [21] and absence of sulfate bands indicates enol type of complexes. The ^{1}H NMR spectrum of $[Zn(OBH–H)_2]$ showed splitting of NH signal as a result of conversion of one of NHC=O to N=C–OH and the existence of the others without participation (Structure 3). The signals of CH_3 protons appeared at the same position as in ligand spectrum. In its ^{13}C NMR, peaks of both ketonic and amidic groups still at the same position with appearance of a new one at 166.21 ppm although one of the $C{=}O_{amidic}$ changed to enol form. Also, the appearance of C=N as doublet peak in 149.44–148.44 ppm range confirming enolization. In the ^{13}C NMR spectrum

Table 3 Elemental analysis and some physical properties of OBH and its complexes

Compound, empirical formula	M.W. (Found, m/e)	Color	M.P. (°C)	Λ (Ohm^{-1} cm^2 mol^{-1})[a]	C % Calcd. (Found)	H % Calcd. (Found)	N % Calcd. (Found)	M % Calcd. (Found)
OBH $C_{10}H_{14}N_4O_4$	254.25 (255.30)	White	247–249	1.76	46.66 (47.04)	5.75 (5.55)	22.70 (22.34)	–
$[Co(OBH)_2Cl]Cl.½EtOH$ $C_{21}H_{31}N_8O_{8.5}Cl_2Co$	661.395	Pale brown	>325	48.0	38.13 (38.13)	4.72 (4.94)	16.94 (16.68)	8.91 (8.63)
$[Zr(OBH)Cl_4]{\cdot}2H_2O$ $C_{10}H_{18}N_4O_6Cl_4Zr$	523.33 (523.4)	Pale orange	>325	20.10	22.95 (22.63)	3.47 (3.87)	10.70 (10.79)	17.70 (17.20)
$[Zn(OBH–H)_2]$ $C_{20}H_{26}N_8O_8Zn$	571.84	Yellowish white	>325	2.62	42.09 (42.49)	4.58 (5.08)	19.59 (19.39)	
$[VO(OBH–H)_2]{\cdot}H_2O$ $C_{20}H_{26}N_8O_{10}V$	591.86	Brown	293	9.74	40.58 (39.99)	4.77 (4.98)	18.93 (18.28)	8.45 (7.93)
$[Cu(OBH)_2Cl_2]{\cdot}2H_2O$ $C_{20}H_{32}N_8O_{10}Cl_2Cu$	678.99	Yellowish green	>325	22.50	35.37 (35.35)	4.45 (4.58)	16.50 (16.07)	9.34 (9.08)
$[Ni_2(OBH)Cl_4]{\cdot}H_2O{\cdot}EtOH$ $C_{20}H_{22}N_4O_6Cl_4Ni_2$	577.62 (371.7)[b]	Reddish brown	>325	37.30	24.95 (24.53)	3.84 (4.11)	9.70 (9.39)	20.34 (20.54)
$[Pd_2(OBH)(H_2O)_2Cl_4]{\cdot}2H_2O$ $C_{10}H_{22}N_4O_4Cl_4Pd_2$	618.18 (620.30)	Brown	>325	24.48	20.63 (20.96)	3.81 (4.20)	9.62 (9.39)	

[a] Molar conductance values for 0.001 mol L^{-1} DMSO solution

[b] The value represents Ni(OBH)Cl·½EtOH

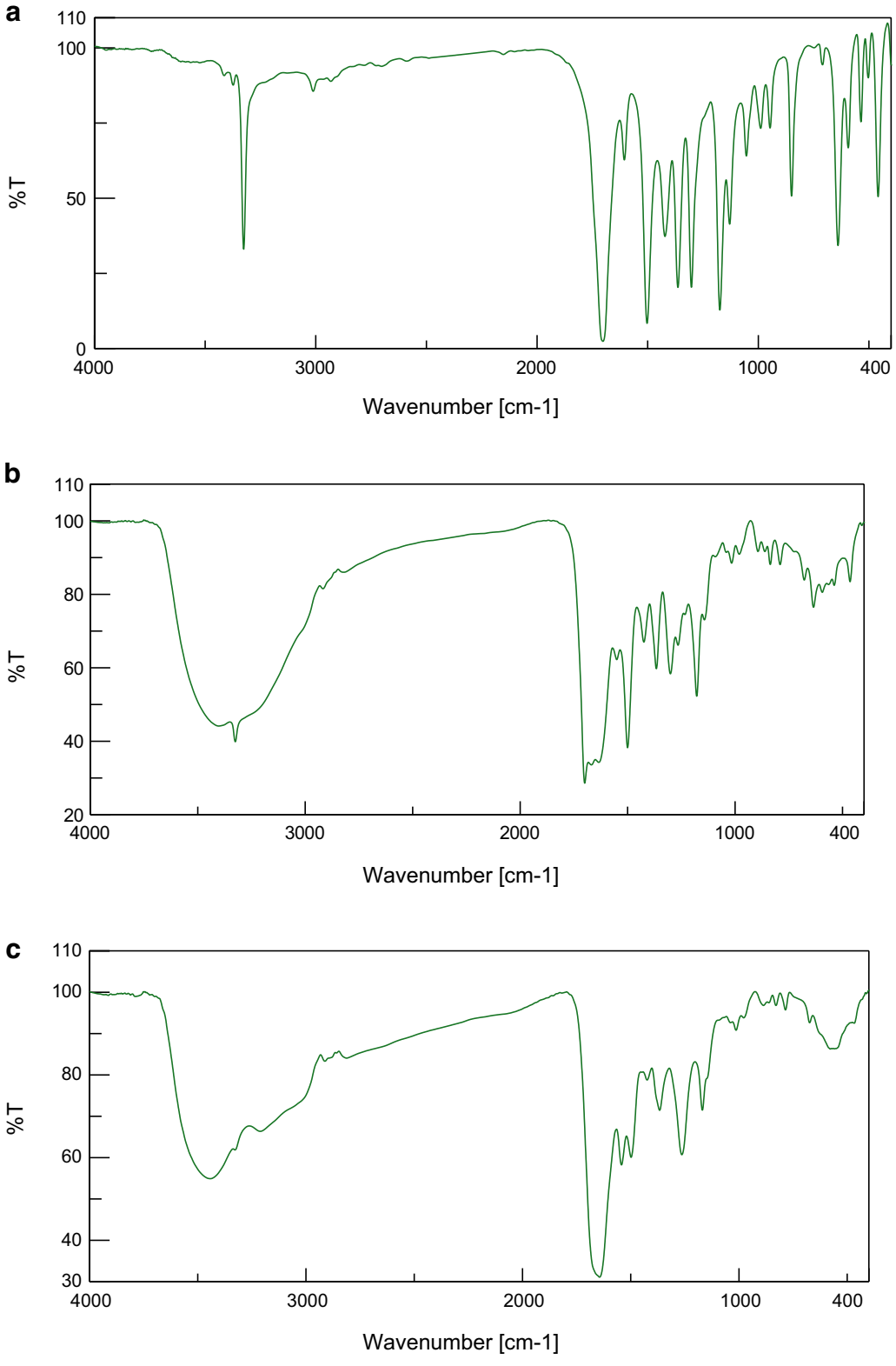

Fig. 1 IR spectra of OBH (**a**); $[Ni_2(OBH)Cl_4]\cdot H_2O\cdot EtOH$ (**b**) and $[Pd_2(OBH)Cl_4]\cdot 6H_2O$ (**c**)

Table 4 IR band assignments of OBH and its complexes

Compound	ν(NH)	ν(C=O)	ν(C=N)	ν(C=N)[a]	ν(C–O)	ν(M–O)	ν(M–N)	Observations
OBH	3325 (s)	1701 (s)	1605 (m)	–	–	–	–	
$[Co(OBH)_2Cl]Cl.½EtOH$	3325 (m)	1699 (s)	1612 (w)	–	–	464 (m)	–	3415 (br) for EtOH
$[Zr(OBH)Cl_4]·2H_2O$	3326 (vbr)[a]	1686 (m)	1585 (m)	–	–	495 (br)	–	
$[Zn(OBH–H)_2]$	–	1699 (s)	1605 (w)	1550 (w)	1140 (w)	463 (s)	–	
$[VO(OBH–H)_2]·H_2O$	–	1696 (s)	1608 (w)	1552 (w)	1142 (w)	463 (m)	–	3412 (br) for H_2O; ν(V=O) at 961
$[Cu(OBH)_2Cl_2]·2H_2O$	3325 (m)	1701 (s)	1610 (br)	–	–	464 (m)	–	3415 (br) for H_2O
$[Ni_2(OBH)Cl_4]·H_2O·EtOH$	3324	1676 (br)	1552 (sh)	–	–	464 (m)	539	3389 (br) for H_2O
$[Pd_2(OBH)(H_2O)_2Cl_4]·2H_2O$	3327 (w)	1644	1542	–	–	467	542	3441 (br) for H_2O

[a] The value for NH and H_2O

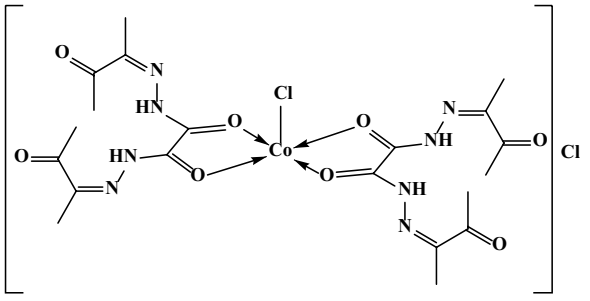

Structure 2 Structure of $[Co(OBH)_2Cl]Cl·½EtOH$

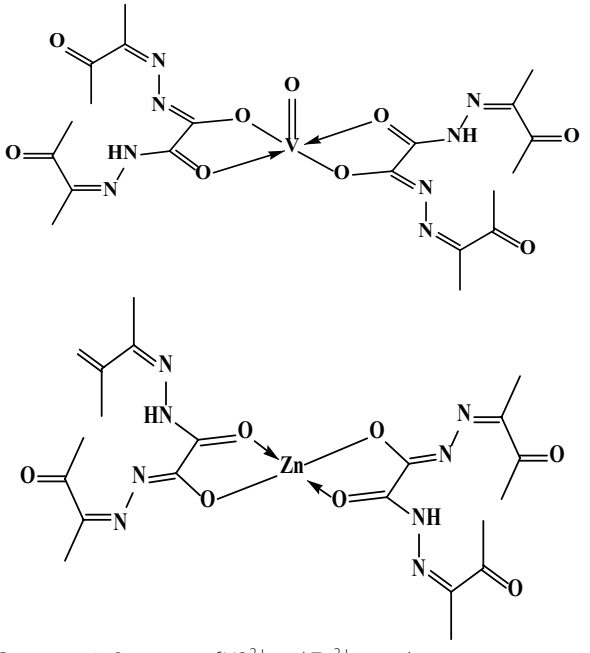

Structure 3 Structures of VO^{2+} and Zn^{2+} complexes

of VO^{2+} complex, the peaks at 172.50, 168.44–167.47, 149.60–148.86, 124.68 and 24.98–24.30 ppm are due to $(C=O)_{ketonic}$, $(C=O)_{amidic}$ free, $(C=O)_{amidic}$ bonded, (C=N), (C=N)*, (C–O) and CH_3, respectively. The appearance of (C=N)* (due to conversion of NHC=O to N*=C–O) and (C–O) peaks confirm enolization process (Table 5).

The third mode confirmed neutral tetradentate but with two metal ions in $[Ni_2(OBH)Cl_4]·H_2O·EtOH$ (Structure 4) and $[Pd_2(OBH)(H_2O)_2Cl_4]·2H_2O$ (Fig. 1b, c). The coordination sites are two azomethine nitrogens of the hydrazone moiety and two carbonyl groups of amidic moiety; each two donors chelated one metal ion. The shift of υ(C=N) to 1542 cm^{-1} and $υ(C=O)_{amidic}$ to 1644 in the Pd(II) complex and to 1552 and 1676 in the Ni(II) complex together with appearance of υ(M–N) [22] and υ(M–O) bands at ~465 and ~540 cm^{-1}, respectively. In the Ni(II) complex, the band of carbonyl groups splitted to two at 1697 and 1676 cm^{-1}; the first is due to ketonic group which is not participated in bonding. The NH band appeared very weak in Ni(II) complex and very broad in Pd(II) complex. Finally, the band at 3389 or 3441 cm^{-1} in Ni(II) or Pd(II) complex is due to hydrated water or ethanol.

Mass spectra

The data of FAB-mass spectra of OBH and some of its complexes are shown in Table 3. The mass spectrum of OBH showed the molecular ion peak (base peak) at m/z = 255.30 (Calcd. 254.25) corresponding to $C_{10}H_{14}N_4O_4$. The peaks shown at 212.2, 190.2, 130.2 and 73.1 are due to $C_8H_{11}N_4O_3$, $C_7H_{11}N_3O_3$, $C_4H_5N_3O_2$ and C_2NO_2.

The mass spectrum of $[Zr(OBH)Cl_4]·2H_2O$ exhibits m/z value of 523.5 (Calcd. 523.33) with 12 % intensity. The value corresponds to $C_{10}H_{18}N_4O_6Cl_4Zr$. Multi-peaks were observed ending with a peak at 69.0 (78 % intensity) may corresponding to 6 C.

Moreover, the mass spectrum of $[Ni_2(OBH)Cl_4]·H_2O·EtOH$ has a value of 371.7 (the base peak) corresponding to Ni(OBH)Cl·½EtOH meaning that this species is highly stable. Multi peaks were observed ending with one at 128.9 (intensity 65 %) due to ZrO_2.

Table 5 ^{1}H and ^{13}C NMR signals of OBH and its diamagnetic complexes

Compound	NH	CH_3	^{13}C signals
OBH	11.924 (s, 2H)	2.129 (s, 6H)	196.65 $(C=O)_{ketonic}$ 167.58; $(C=O)_{amidic}$ 148.81 (C=N) 23.90 (CH_3)
$[Zn(OBH–H)_2]$	11.781 (s, 1H) 11.565 (s, 1H)	2.371 (s, 3H) 2.118 (s, 3H)	196.68 $(C=O)_{ketonic}$ 168.02 $(C=O)_{amidic}$ free 166.21 $(C=O)_{amidic}$ bonded 149.44 (C=N), (C=N)* 23.94 (CH_3)
$[VO(OBH-H)_2]\cdot H_2O$	11.769 (s, 1H)	2.087 (s, 3H) 2.053 (s, 3H)	197.12 $(C=O)_{ketonic}$ 172.50 $(C=O)_{amidic}$ (free) 168.44–167.47 $(C=O)_{amidic}$ (bonded) 149.60–148.86 (C=N), (C=N)* 124.68 (C–O) 24.68; 24.98 (CH_3)
$[Pd_2(OBH)(H_2O)_2Cl_4]\cdot 2H_2O$	11.766 (s, 1H) 11.566 (s, 1H)	2.290 (s, 6H)	196.75 $(C=O)_{ketonic}$ 167.98; $(C=O)_{amidic}$ 148.88 (C=N) 22.90 (CH_3)

*New azomethine group as a result of enolization

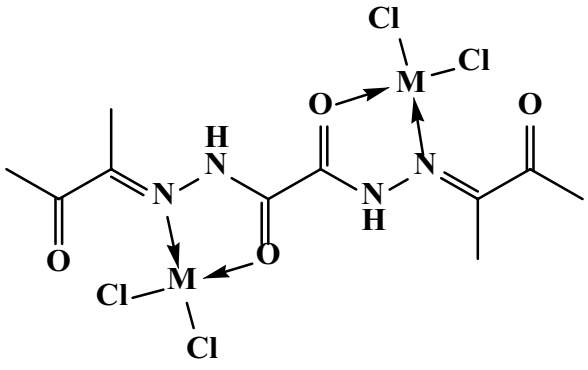

Structure 4 Structure of $[Ni_2(OBH)Cl_4]\cdot H_2O\cdot EtOH$

Magnetic moments and electronic spectra

The electronic spectral bands of the complexes as well as the magnetic moment values are presented in Table 6. The DMSO solutions of complexes have the same color as in the solid complexes. OBH exhibits one absorption band at 38,460 cm^{-1} collectively due to $\pi \rightarrow \pi^*$ transitions of C=N, $C=O_{ketonic}$ and $C=O_{amidic}$ groups [23]. The broadness of the band may be due to existence of these groups in opposite sides. The two bands at 25,510 and 23,810 cm^{-1} in Cu(II) complex may be due to N → MCT and O → MCT [24]. The Ni(II) complex has only one band at 28,330 cm^{-1} due to N → MCT while Co(II) and Zr(IV) have also one band but at 23,320 and 22,830 cm^{-1}, respectively, due to O → MCT.

Table 6 Magnetic moments, electronic spectra and molar extension coefficient of OBH and its complexes

Compound	μ_{eff} (BM)	Intraligand and charge transfer transition, cm^{-1} (*ε)	d–d transition cm^{-1} (*ε)	Proposed structure
OBH	–	38,460 (790)	–	
$[Co(OBH)_2Cl]Cl\cdot ½EtOH$	2.51	37,450 (195.8); 23,320 (115.8)	15,250 (94)	Square-pyramid
$[Zr(OBH)Cl_4]\cdot 2H_2O$	–	36,495 (399); 22,830 (117.6)	–	Octahedral
$[Zn(OBH–H)_2]$	–	37,450 (530); 35,335 (885)	–	Tetrahedral
$[VO(OBH–H)_2]\cdot H_2O$	0.00	38,060; 35,040; 29.210		Square-pyramid
$[Cu(OBH)_2Cl_2]\cdot 2H_2O$	1.45	39,840; 37,590; 25,510; 23,810 (350)	20,080	Octahedral
$[Ni_2(OBH)Cl_4]\cdot H_2O\cdot EtOH$	1.36[a]	39,840; 37,590; 28,330	19,050	Square-planar + tetrahedral
$[Pd_2(OBH)(H_2O)_2Cl_4]\cdot 2H_2O$	0.00	37,540; 28,470	21,500 (310)	Square-pyramid

*ε is the molar extension coefficient (mol^{-1} L)

[a] The value per one nickel atom

$[Co(OBH)_2Cl]Cl{\cdot}½EtOH$ (pale brown) has 2.51 BM magnetic moment which lies within the values reported for one unpaired electron of square-planar or square-pyramid Co(II) complexes [25] having dsp^2 or dsp^3 hybridization. Evidence is electronic spectrum which showed one band at 15,250 cm^{-1} with molar extension coefficient of 94 mol^{-1} L. The spectrum resembled the spectra of the five-coordinate Co(II) complexes [26] and the square-pyramid is the suggested geometry.

The magnetic moment value, for each atom, in $[Ni_2(OBH{-}2H)Cl_4]{\cdot}H_2O{\cdot}EtOH$ is 1.36 BM which is less than the normal values reported for tetrahedral or octahedral coordination containing two unpaired electrons. Its electronic spectrum showed a broad band at 19,050 cm^{-1} ($\varepsilon = 180$ mol^{-1} L) typical of a square-planar structure with some distortion [26] may be of tetrahedral; the anomalous magnetic value is consistent with mixed stereochemistry (square-planar + tetrahedral) around the two nickel ions [27]. On the other hand, the diamagnetic nature of $[Pd_2(OBH)(H_2O)_2Cl_4]{\cdot}2H_2O$ proved the square-pyramid structure in which the metal is surrounded by NO donors, two chloro and one coordinated water. The bands at 37,540 and 28,470 cm^{-1} are attributed to charge transfer transitions, probably O → Pd transition [28].

The electronic spectrum of $[Cu(OBH)_2Cl_2]{\cdot}H_2O$ exhibits one band with maximum at 20080 cm^{-1} assigned to the $^2E_{2g} \rightarrow {}^2T_{2g}$ transition in an octahedral geometry [29]. The band is broad due to the Jhan-Teller effect which enhances the distortion of the octahedral geometry generally important for odd number occupancy of the e_g level. The magnetic moment value (1.45 BM) was found lower than the values reported for the d^9–system containing one unpaired electron (1.73–2.25 BM) suggesting interactions between the copper centers.

Table 7 Decomposition steps of the complexes based on the thermogravimetric data

Complex	DTG maximum temp. (°C)	Removing species	Weight loss % Found (Calcd)
$[Co(OBH)_2Cl]Cl{\cdot}½EtOH$	60	- $½Cl_2 + ½EtOH$	6.36 (8.84)
	319	- $C_{16}H_{24}N_4O_6Cl$	60.45 (61.05)
	500	- $C_4H_4N_2$	11.77 (12.11)
	>500	$[CoO_4N_2]$ (residue)	21.58 (22.82)
$[Zr(OBH)Cl_4]{\cdot}2H_2O$	76	- $(Cl_2 + H_2O)$	16.12 (16.99)
	313	- $(H_2O + C_8H_{12}N_2O_2)$	37.67 (35.58)
	449	- Cl_2	12.44 (13.55)
	>500	$C_2N_2O_2Zr$ (residue)	30.15 (33.67)
$[VO(OBH\text{-}H)_2]{\cdot}H_2O$	59	- H_2O	3.65 (3.04)
	289	- $C_{16}H_{24}N_4O_6$	61.57 (62.24)
	405–590	- $C_4H_4N_4O_2$	25.56 (23.67)
	>600	V (residue)	7.45 (8.53)
$[Cu(OBH)_2Cl_2]{\cdot}2H_2O$	59	- $2H_2O$	4.29 (5.31)
	291	- $C_{16}H_{24}N_4O_6$	54.90 (54.26)
	374	- $C_4H_4N_4O_3$	25.56 (26.37)
	>400	CuO (residue)	12.30 (11.71)
$[Ni_2(OBH)Cl_4]{\cdot}H_2O{\cdot}EtOH$	72	- $(EtOH + H_2O)$	13.51 (11.08)
	368	- $(Cl_2 + C_8H_{12}N_2O_2)$	40.20 (41.40)
	470	- Cl_2	11.20 (12.27)
	550	- $C_2H_2N_2$	8.00 (9.35)
	>600	2 NiO (residue)	27.09 (25.87)
$[Pd_2(OBH)(H_2O)_2Cl_4]{\cdot}2H_2O$	75	- $2H_2O$	6.47 (5.83)
	322	- $2H_2O + 2Cl_2 + C_4H_{12}$	38.49 (38.48)

Thermal analysis

The decomposition steps, the DTG maximum temperature and the removing species are shown in Table 7. The thermogram of $[Co(OBH)_2Cl]Cl{\cdot}½EtOH$ showed three decomposition steps at mid- points of 60, 319 and 500 °C corresponding to the removal of $½Cl_2 + ½EtOH$ (Found 6.36 %; Calcd. 8.84 %); $C_{16}H_{24}N_4O_6Cl$ (Found 60.45 %; Calcd. 61.05 %) and $C_4H_4N_2$ (Found 11.77 %; Calcd 12.11 %) leaving $[CoO_4N_2]$ moiety (Found 21.58 %; Calcd. 22.82 %).

The TG curve of $[VO(OBH\text{-}H)_2]{\cdot}H_2O$ showed also three steps; the first (mid. point 56 °C) represents the removal of the outside water molecule (Found 3.65 %; Calcd 3.04 %); the second (mid. point 289 °C) represents the loss of $C_{16}H_{24}N_4O_6$ (Found 61.57 %; Calcd 62.24 %) and the third for the repulsion of $C_4H_4N_4O_2$ (Found 25.56 (Calcd. 23.67 %). The residue is vanadium metal (Found 7.45; Calcd 8.53 %).

$[Cu(OBH)_2Cl_2]{\cdot}2H_2O$ thermogram showed decomposition steps ending with copper oxide at Temp. >400 °C. The decomposition showed the removal of the two hydrated water in the first step at mid. point of 59 °C. The other two steps were observed at 291 and 374 °C corresponding to the removal of $C_{16}H_{24}N_4O_6$ and $C_4H_4N_4O_3$, respectively, leaving CuO as a residue.

The TG curve of $[Ni_2(OBH)Cl_4]{\cdot}H_2O{\cdot}EtOH$ showed four steps. The first at 72 °C is due to the removal of the outside water and EtOH (Found 13.51 %; Calcd. 11.08 %). The second step (368 °C) represents the loss of $Cl_2 + C_8H_{12}N_2O_2$ (Found 40.20 %; Calcd 41.40 %). The third step represents the repulsion of Cl_2 (Found 11.20 %; Calcd. 12.27 %). The fourth step (Found 8.00 %; Calcd. 9.35 %) corresponding to the removal of $C_2H_2N_2$. The residue is 2NiO (Found 27.09 %; Calcd. 25.87 %) (Fig. 2).

The thermogram of $[Zr(OBH)Cl_4]{\cdot}2H_2O$ has $C_2N_2O_2Zr$ as remaining residue above 500 °C with 30.15 % (Calcd. 33.67 %). The first three steps observed at mid. points of 76, 313 and 449 °C are corresponding to the removal of

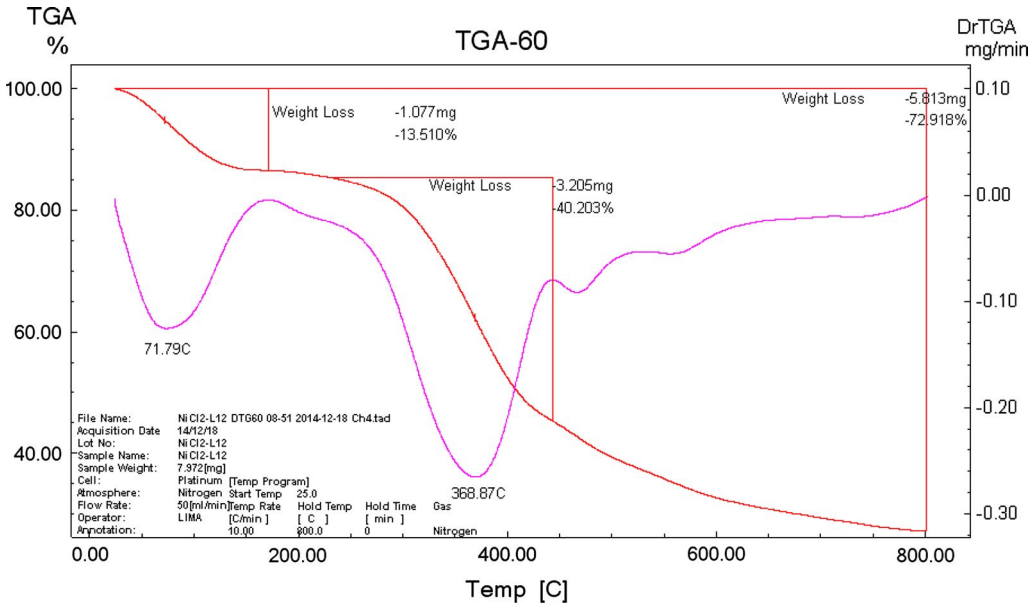

Fig. 2 TGA thermogram of $[Ni_2(OBH)Cl_4]\cdot H_2O\cdot EtOH$

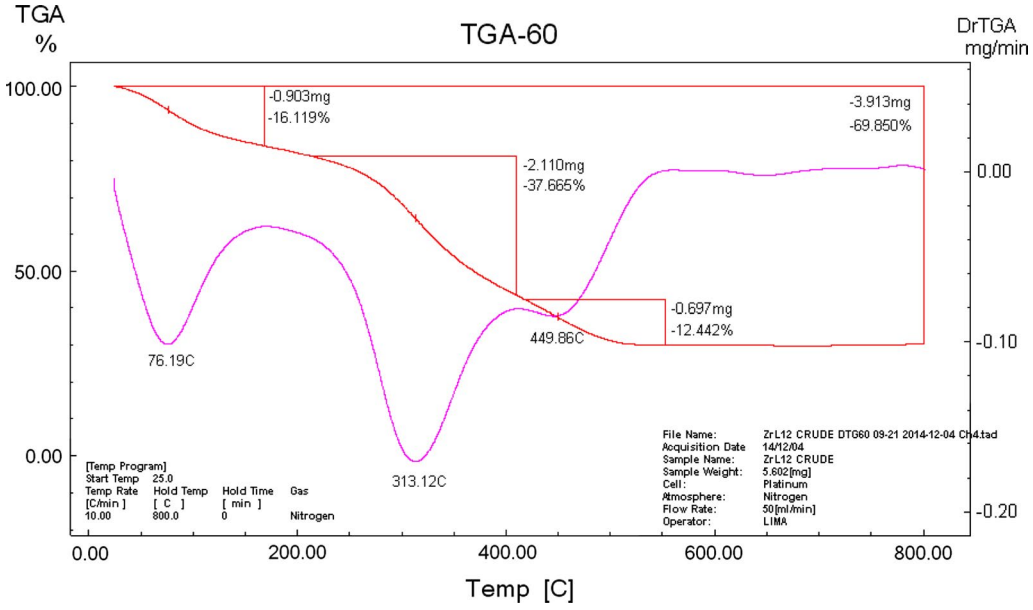

Fig. 3 TGA thermogram of $[Zr(OBH)Cl_4]\cdot 2H_2O$

$(Cl_2 + H_2O)$; $(H_2O + C_8H_{12}N_2O_2)$ and Cl_2, respectively (Fig. 3).

The thermogram of $[Pd_2(OBH)(H_2O)_2Cl_4]\cdot 2H_2O$ showed two main steps at 75 and 322 °C due to the liberation of the outside water and $2H_2O + 2Cl_2 + C_4H_{12}$, respectively. High residue % was found over 500 °C.

Molecular modeling

Trials to grow single crystals for the investigated complexes were failed. In order to calculate the molecular parameters, $[Co(OBH)_2Cl]Cl\cdot ½EtOH$ and $[Ni_2(OBH)Cl_4]\cdot H_2O\cdot EtOH$ (Structure 5) are chosen and their data are presented in Table 8. The bond lengths and the bond

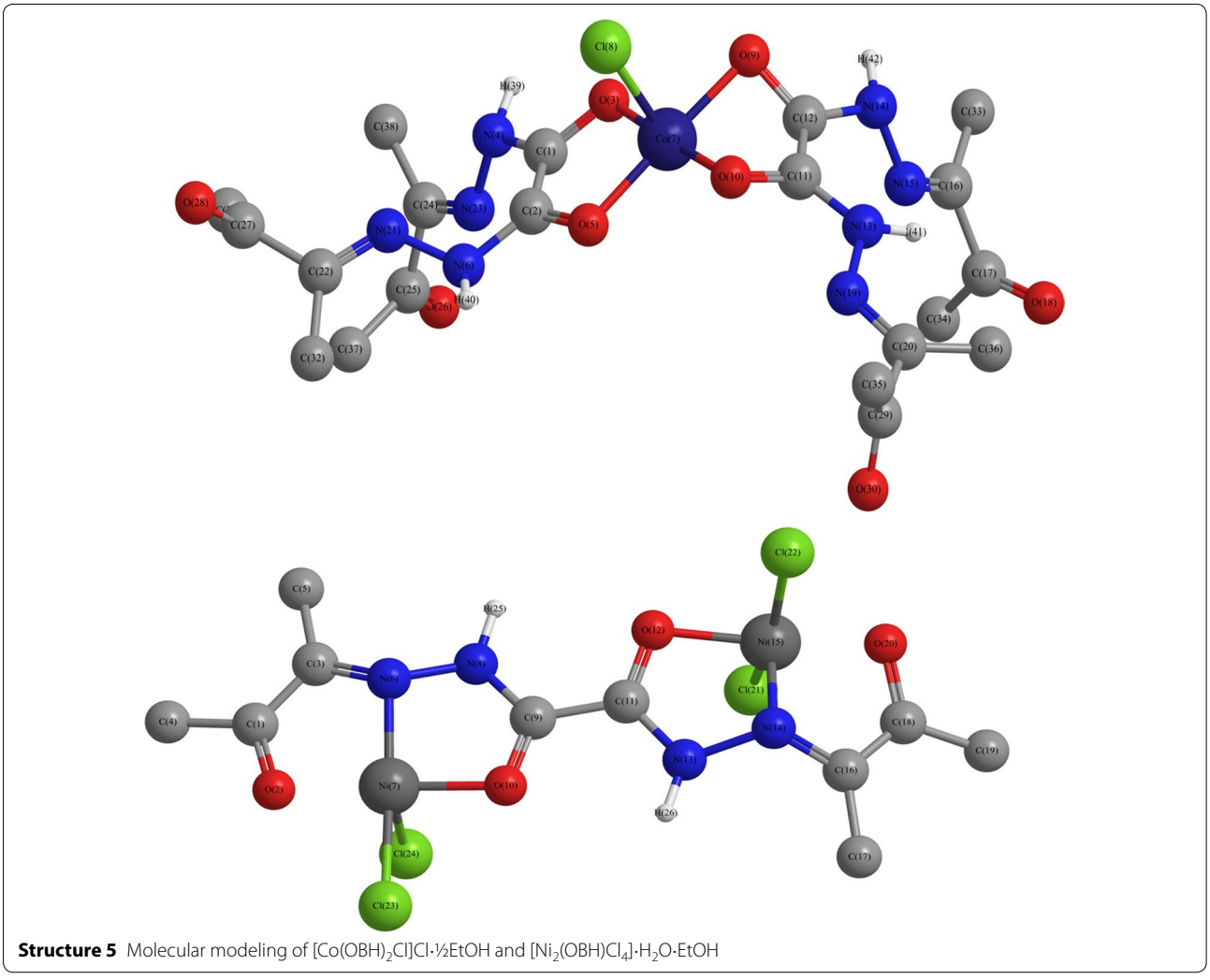

Structure 5 Molecular modeling of $[Co(OBH)_2Cl]Cl{\cdot}½EtOH$ and $[Ni_2(OBH)Cl_4]{\cdot}H_2O{\cdot}EtOH$

Table 8 Molecular parameters of the Co(II) and Ni(II) complexes

Parameter	$[Co(OBH)_2Cl]Cl{\cdot}½EtOH$	$[Ni_2(OBH)Cl_4]{\cdot}H_2O{\cdot}EtOH$
Total energy (kcal/mol)	−174051.6072885	−151380.5229794
Total energy (a.u.)	−277.368857336	−241.240189251
Binding energy (kcal/mol)	−6649.8942255	−3610.0626914
Isolated atomic energy (kcal/mol)	−167401.7130630	−147770.4602880
Electronic energy (kcal/mol)	−1559859.4974432	−935598.9682580
Core–core interaction (kcal/mol)	1385807.8901548	784218.4452785
Heat of formation (kcal/mol)	−261.3762255	−159.9386914
Gradient (kcal/mol/Å)	53.4569309	42.0607388
Dipole (Debyes)	4.949	0.413

angles are shown in Additional file 1: Tables S1 and S2. It is obvious that the energy values obtained for $[Ni_2(OBH)Cl_4]{\cdot}H_2O{\cdot}EtOH$ are less than those of $[Co(OBH)_2Cl]Cl{\cdot}½EtOH$ indicating that the presence of two metals stabilized the complex more than the mono metal lowering the energy. The dipole moment calculated for the Co(II) complex is 4.949 D proving the polar nature of the complex. The value of Ni(II) complex is 0.413 D indicating its non-polarity.

Biological activity

The antimicrobial activity of the metal complexes depends on the following factors: the chelate effect, i.e., bidentate ligands show higher antimicrobial activity than monodentate; the nature of the ligands; the total charge of the complex: cationic > neutral > anionic; the nature of the counter ion and the nuclearity of the metal center: binuclear are more active than mononuclear ones. It depends more on the metal center itself than on the geometry around the metal ion.

The antimicrobial activities of OBH and its complexes are examined against *Bacillus, E. coli, Aspergillus,*

Table 9 Effect of ligand and its complexes on some microorganisms

Compound	*Bacillus*	*E. coli*	*Aspergillus*	*Penicillium*	*Fusarium*
OBH	Nil	2.0	Nil	Nil	Nil
$[Co(OBH)_2Cl]Cl{\cdot}½EtOH$	Nil	1.0	Nil	Nil	15
$[Zr(OBH)Cl_4]{\cdot}2H_2O$	10	Nil	4.0	9.0	8.0
$[Zn(OBH–H)_2]$	Nil	1.0	Nil	Nil	5.0
$[Cu(OBH)_2Cl_2]{\cdot}2H_2O$	Nil	2.0	Nil	5.0	Nil
$[Ni_2(OBH)Cl_4]{\cdot}H_2O{\cdot}EtOH$	Nil	2.0	Nil	Nil	Nil
$[Pd_2(OBH)(H_2O)_2Cl_4]{\cdot}2H_2O$	Nil	Nil	Nil	Nil	5.0
$[VO(OBH–H)_2]{\cdot}H_2O$	Nil	Nil	Nil	Nil	5.0
DMSO	Nil	Nil	Nil	Nil	Nil
Ampicillin	25	–	27	–	–
Gentamicin	–	48	20	25.9	–

Reading in diameter (mm)

Penicillium and Fusarium and the data are given in Table 9. The data showed that $[Zr(OBH)Cl_4]{\cdot}2H_2O$ has higher activity against all tested microorganisms except *E. coli*. The activity is highest and more with *Penicillium* (9 mm zone inhibition). The higher activity may be due the presence of non-ionizable chlorine and to the less planarity of the complex making it more lipophilic. Most compounds have high activity against *Fusarium*. $[Cu(OBH)_2Cl_2]{\cdot}2H_2O$ has higher value against *Fusarium* (15 mm). Comparing these data with that of ampicillin and those obtained for different hydrazone complexes showed more or less activity [29, 30].

Conclusion

Oxalo bis(2,3-butanedionehydrazone) has been prepared and characterized by x-ray crystallography. It coordinates as neutral bidentate; mononegative bidentate and neutral tetradentate. The complexes have tetrahedral, square-planar and/or octahedral structures. The VO^{2+} and Co^{2+} complexes have square-pyramid structure. $[Cu(OBH)_2Cl_2]{\cdot}2H_2O$ and $[Ni_2(OBH)Cl_4]{\cdot}H_2O{\cdot}EtOH$ decomposed to their oxides while $[VO(OBH–H)_2]{\cdot}H_2O$ to the metal. The energies from molecular modeling calculation is less in $[Ni_2(OBH)Cl_4]{\cdot}H_2O{\cdot}EtOH$ than those for $[Co(OBH)_2Cl]Cl{\cdot}½EtOH$ indicating that the presence of two metals stabilized the complex more than the mono metal. The Co(II) complex is polar molecule while the Ni(II) is non-polar.

Further materials

Crystallographic data for the structure reported in this paper have been deposited with Cambridge Crystallographic Data Center as supplementary publication CCDC-985982.

Additional file

Additional file 1: Table S1. Bond lengths and bond angles of the Ni(II) complex. **Table S2.** Bond lengths and bond angles of the Co(II) complex.

Authors' contributions

MA and AES do the experimental part; AEA and BJ interpreted the results and wrote the manuscript. All authors read and approved the final manuscript.

Acknowledgements

This work was supported and funded by Kuwait University Research Grant for the Project SC05/14. The authors acknowledge all service labs in the Faculty of Science, Kuwait University (GS 01/01; GS 01/03; GS 01/05; GS 03/08).

Competing interests

The authors declare that they have no competing interests.

Received: 4 June 2015 Accepted: 1 October 2015
Published online: 29 December 2015

References

1. Despaigne AR, Parrilha GL, Izidoro JB, da Costa PR, dos Santos RG, Piro OE, Castellano EE, Rocha WR, Beraldo H (2012) 2-Acetylpyridine- and 2-benzoylpyridine-derived hydrazones and their gallium(III) complexes are highly cytotoxic to glioma cells. Eur J Med Chem 50:163
2. Ranford JD, Vittal JJ, Wang YM (1998) Dicopper(II) complexes of the antitumor analogues acylbis(salicylaldehydehydrazones) and crystal structures of monomeric [Cu(2)(1,3-propanedioyl bis(salicylaldehydehydrazone))(H(2)O)(2)]. (ClO(4))(2)·3H(2)O and Polymeric-[{Cu(2)(1,6hexanedioylbis(salicylaldehydehydrazone))(C(2)H(5)OH)(2)}(m)()]. (ClO(4))(2)(m)()·m(C(2)H(5)OH). Inorg Chem 37(6):1226
3. El-Asmy AA, Khalifa MI, Hassanian MM (2001) Synthesis and spectroscopic studies on novel transition metal complexes of 3-oximino-3-(2-pyridylcarbamoyl) propane-2-one. Synth React Inorg Met Org Chem 31(10):1787
4. Jayawant AM, Stephenson RE, Ralph JD (1999) 2,3-Butanedione monoxime cardioplegia: advantages over hyperkalemia in blood-perfused isolated hearts. Ann Thorac Surg 67:618
5. Shallaby AM, Mostafa MM, Ibrahim KM, Moussa MNH (1984) New uranyl(VI) complexes with hydrazone-oximes derived from aromatic acid hydrazides and biacetylmonoxime. Spectrochim Acta 40A:999
6. Showalter HDH, Johnson JL, Hoftiezer JM et al (1987) Anthrapyrazole anticancer agents. Synthesis and structure-activity relationship against murine leukemias. J Med Chem 30:121
7. Rostom SAF, Shalaby MA, El-Demellawy MA (2003) Polysubstituted pyrazoles—part 5. Synthesis of new 1-(4-chlorophenyl)-4-hydroxy-^{1}H-pyrazole-3-carboxylic acid hydrazide analogs and some derived ring systems. A novel class of potential antitumor and anti-HCV agents. Eur J Med Chem 38:959
8. El-Asmy AA, Khalifa MI, Rakha TH, Hassanian MM, Abdallah AM (2000) Mono and trinuclear complexes of oximinoacetoacetyl-pyridine-4-phenylthiosemicarbazone. Chem Pharm Bull 48(1):41
9. Latha KP, Vaidya VP, Keshavayya J (2004) Comparative studies on metal complexes of 2-acetylnaphtho[2,1-b]furan oxime and 2-benzoylnaphtho[2,1-b]furan Oxime. Synth React Inorg Met Org Chem 34:667
10. El-Asmy AA, Khalifa MI, Hassanian MM (2004) Synthesis and characterization of transition metal complexes containing oxime, amido and thioamido groups. Ind J Chem 43A:92
11. Al-Gammal OA, El-Asmy AA (2008) Synthesis and spectral characterization of 1-(amino-N-phenylform)-4-ethylthiosemicarbazide and its metal complexes. J Coord Chem 61(14):2296

12. Nandy M, Hughes DL, Rosair GM, Singh RKB, Mitra S (2014) Synthesis, characterization, crystal structure and DNA binding of two copper(II)–hydrazone complexes. J Coord Chem 67(20):3335
13. West DX, Ives JS, Bain GA, Liberta AE, Martiniz J, Ebert KH (1997) Copper(II) and nickel(II) complexes of 2,3-butanedione bis(N(3)-substituted thiosemicarbazones). Polyhedron 16:1895
14. El-Sayed AEM, Al-Fulaij OA, Elaasar A, El-Defrawy MM, El-Asmy AA (2015) Spectroscopic characterization and biological activity of dihydrazone complexes: crystal structure of 2,3-butanedione bis(isonicotinyl-hydrazone). Spectrochim Acta 135A:211
15. El-Tabl AS, El-Saied FA, Plass W, Al-Hakimi AN (2008) Synthesis, spectroscopic characterization and biological activity of the metal complexes of the Schiff base derived from phenylaminoacetohydrazide and dibenzoylmethane. Spectrochim Acta 71A:90
16. Jeragh B, El-Asmy AA (2014) Spectroscopic and structural study of some 2,5-hexanedione bis(salicyloylhydrazone) complexes: crystal structures of its Ni(II) and Cu(II) complexes and N-(2,5-dimethyl-1H-pyrrol-1-yl)-2-hydroxybenzamide. Spectrochim Acta 129A:307
17. Al-Fulaij OA, Jeragh BM, El-Sayed AE, El-Defrawy MM, El-Asmy AA (2015) Chelation, spectroscopic characterization and crystal structure of 2,3-butanedione isonicotinylhydrazone: determination of Zr^{+4} after flotation separation. Spectrochim Acta 136A:1834
18. Geary WJ (1971) The use of conductivity measurements in organic solvents for the characterisation of coordination compounds. Coord Chem Rev 7:81
19. Jeragh B, El-Asmy AA (2014) Coordination of Fe(III), Co(II), Ni(II), Cu(II), Zn(II), Cd(II), Hg(II), Pd(II) and Pt(II) with 2,5-hexanedione bis(thiosemicarbazone), HBTS: crystal structure of cis-[Pd(HBTS)]Cl_2 and 1-(2,5-dimethyl-1H-pyrrol-yl)-thiourea. Spectrochim Acta 130A:546
20. El-Asmy AA, El-Gammal OA, Saleh H (2008) Spectral, thermal, electrochemical and analytical studies on Cd(II) and Hg(II) thiosemicarbazone complexes. Spectrochim Acta 71A:39
21. Kumar A, Prasad R, Kociok-Köhn G, Molloy KC, Singh N (2009) Synthesis, crystal structures and properties of sterically congested heteroleptic complexes of group 10 metal ions with p-tolyl sulphonyl dithiocarbimate and 1,2-bis (diphenylphosphino)ethane. Inorg Chem Commun 12:686
22. Patel M, Patel C, Joshi H (2013) Metal-based biologically active compounds: synthesis, characterization, DNA interaction, antibacterial, cytotoxic and SOD mimic activities. Appl Biochem Biotechnol 169:1329
23. West DX, El-Sawaf AK, Bain GA (1998) Metal complexes of N(4) substituted analogs of antiviral drug methisazone (1-methylisatin) thiosemicarbazones. Transit Met Chem 23:1
24. Downes JM, Whelan J, Bosnich B (1981) Inorganic reactions and methods. Inorg Chem 20:1081
25. Ketcham KA, Swearingen JK, Castineiras A, Garcia I, Bermejo E, West DX (2001) Iron(III), cobalt(II, III), copper(II) and zinc(II) complexes of 2-pyridineformamide 3-piperidylthiosemi-carbazone. Polyhedron 20:3265
26. Amer S, El-Wakiel N, El-Ghamry H (2013) Synthesis, spectral, antitumor and antimicrobial studies on Cu(II) complexes of purine and triazole Schiff base derivatives. J Mol Strut 1049:326
27. Lehmann U, Lach J, Loose C, Hahn T, Kersting B, Kortus J (2013) Binuclear nickel complexes with an edge sharing bis(square-pyramidal) $N_3Ni(\mu\text{-}S_2)NiN_3$ core: synthesis, characterization, crystal structure and magnetic properties. J Dalton Trans 42:987
28. Perera SD, Fernandez-Sanchez JJ, Shaw BL (2001) Activation of C–X (X=Cl or Br) bonds in 2-halobenzaldehydes as their 2-pyridylhydrazone derivatives: oxidative addition to tungsten(0) to give aryl–tungsten(II) complexes. Inorg Chim Acta 325:175
29. Amendola V, Boiocchi M, Brega V, Fabbrizzi L, Mosca L (2010) Octahedral copper(II) and tetrahedral copper(II) double-strand helicates: chiral self-recognition and redox behavior. Inorg Chem 49:997
30. El-Dissouky A, Al-Fulaij O, Awad MK, Rizk S (2010) Synthesis, characterization, and biological activity studies of copper(II)–metal(II) binuclear complexes of dipyridylglyoxal *bis*(2-hydroxybenzoyl hydrazone). J Coord Chem 63:330